DOI:
10.1007/s10875-023-01491-x

Document Version
Peer reviewed version

Novel *NFKB2* pathogenic variants in two unrelated patients with common variable immunodeficiency

Kruthika Sundaram* [1,2], Micol Ferro* [1,2], Inborn Errors of Immunity Functional Diagnostics Consortium[†], Grant Hayman [3], Mohammad A A Ibrahim[1]

Correspondence: m.ibrahim@kcl.ac.uk

1 King's College London, King's Health Partners, King's College Hospital NHS Foundation Trust, School of Immunology and Microbial Sciences, Department of Immunological Medicine, Denmark Hill, London SE5 9RS, UK

2 Viapath, King's College Hospital, Denmark Hill, London SE5 9RS, UK

3 Epsom & St Helier University Hospitals NHS Trust, Carshalton, SM5 1AA, UK

* Equally contributed to this manuscript

† A list of members and their affiliations is shown at the end of the manuscript

KEYWORDS: Common Variable Immunodeficiency (CVID), *NFKB2*, novel pathogenic gene variants, *lym1* mice, hypogammaglobulinaemia, autoimmunity

To the Editor

Common Variable Immunodeficiency (CVID) is a heterogeneous group of primary antibody deficiencies varying both phenotypically and genetically. Hallmark features include recurrent sinopulmonary bacterial infections, hypogammaglobulinaemia and impaired functional antibody responses, with additional comorbidities such as granulomatous disease and autoimmune features in some patients[1]. We present two unrelated cases with hypogammaglobulinaemia, recurrent infections and alopecia areata. At the time of investigation, Patient 1 was a 26-year-old male and patient 2, a 36-year-old female, both with recurrent infections since childhood receiving immunoglobulin replacement therapy subcutaneously. Additionally, Patient 1 was on oral hydrocortisone replacement therapy following the diagnosis of central adrenal insufficiency (low plasma cortisol and adrenocorticotropic hormone, ACTH). The salient clinical features and laboratory findings of the patients are summarised in **Table S1**.

It has been estimated that approximately 2-10% of CVID patients have a monogenic cause of the disease, and of these, 5% have pathogenic variants in the nuclear factor kappa-B subunit-2 gene (*NFKB2*) that encodes the p100 subunit of the transcription factor complex NFκB and is a key player in the noncanonical NFκB signalling pathway[1], **Fig. 1A** is a diagrammatic representation of NFκB (p100) protein domains showing the Rel homology domain (RHD), ankyrin repeat domain (ARD) and death domain (DD). Multiple alignments of homologous/orthologous sequences are displayed, with three highlighted serine residues (S866, S870 & S872) that are highly conserved among species. Noncanonical NFκB pathway stimulation triggers a cascade of events that lead to p100 processing to p52 and nuclear translocation of RelB/p52 heterodimer that initiates the transcription of target genes[2]. The first crucial event in the

noncanonical NFκB signalling pathway is the signal-induced accumulation of NFκB inducing kinase (NIK) that, together with IκB kinase α (IKKα), phosphorylates p100. The conserved serine residues S866 and S870 are the major phosphorylation sites essential for the processing of p100 to p52 in cells. IKKα phosphorylates the conserved serine S872 *in vitro*. However, inducible cellular processing of p100 is not dependent on S872. The two major phospho-serines (S866 & S870) create a binding site for β-TrCP, the receptor subunit of the E3 ubiquitin ligase β-TrCP^{SCF}, which mediates p100 ubiquitination and its proteasomal-dependent processing to p52 employing the p100 ubiquitin acceptor site lysine 855[3].

ACTH deficiency and alopecia areata are complications in CVID patients that have been associated with pathogenic variants in the *NFKB2*[1,4]. We postulated that in these two unrelated cases with similar complications, there was a causative defect in *NFKB2*. Sanger sequencing (**Fig. 1B**) identified two different novel heterozygous genetic variants at position 2604 in the cDNA of the patients (Patient 1: c.2604C>G; patient 2: c.2604C>A; RefSeq NM_001077494.3), creating in both cases a premature STOP codon due to pathogenic nonsense variants (Patient 1: TAG; patient 2: TAA). The translation of p100 was predicted to terminate at amino acid position 868, truncating 33 amino acids from the C-terminal end (p.Tyr868*, **Fig. 1A**). The unaffected family members (**Fig. 1C**) of Patient 1 have two wild-type alleles (**Fig.1B** – the sequence of the mother of Patient 1 is shown as reference) of the gene and normal immunoglobulin levels (data not shown), indicating that the variant in Patient 1 is a likely *de novo* pathogenic variant (**Fig. 1B**). Information regarding the family of patient 2 is unavailable.

CD40L stimulation of peripheral blood mononuclear cells (PBMCs) predominantly activates the noncanonical NFκB signalling pathway in cells with surface CD40, leading to the phosphorylation of p100 and its consequent processing to p52. Immunoblot analysis of whole cell

lysates of PBMCs, upon stimulation with CD40L, showed impaired processing of p100 to p52 in Patient 1 compared to his family members who were our healthy donors (HD 1 and HD 2). The reduction of p100 processing was linked to a markedly less increased phosphorylation of p100 in Patient 1 compared to the controls – which is likely caused by the absence of S870 in the p100 truncated form (p.Tyr868*). Patient 1 expressed both full-length p100 (from the wild-type allele) and the truncated form (from the mutant allele), which are both visible in **Fig. 2A (top panel)**; p100(p.Tyr868*) had increased electrophoretic mobility and created an additional 93kDa band. In CD40L-stimulated PBMCs from the patient, the truncated p100 (p.Tyr868*, 93kDa) accumulated unprocessed compared with the unstimulated cells (**Fig. 2A, top panel)**, indicating that this variant produces a C-terminal-truncated p100(p.Tyr868*) that causes an excess of unprocessable p100 (and therefore an excess of IκB-like activity) and reduce the amount of processed p52. In CD40L-stimulated cells from both HD1 and HD2, p100 was efficiently processed to p52 compared with unstimulated cells (**Fig. 2A, top panel**). A limitation of this finding could be the B lymphopenia in Patient 1 (**Table S1**). Purification of B cells was not practical due to the low numbers in Patient 1. However, we confirmed our results using lymphoblastoid cell lines (LCLs). CD40L stimulation of LCLs derived from Patient 1 showed accumulation of truncated p100(p.Tyr868*) and reduced processing to p52 in contrast to LCLs from HD1 and HD2 (**Fig. 2B, top panel**). The dominance of the truncated p100(p.Tyr868*) upon stimulation with CD40L of LCLs from the patient may be due to a shorter period of stimulation of LCLs compared with PBMCs, and the effect of IκB-like activity due to the accumulation of the truncated p100. In addition to S866/S870 phosphorylation, we analysed phosphorylation of only S870, which is absent in the truncated p100 of Patient 1. Immunoblotting our patient's LCLs with the antibody specific to S870 revealed a much dimmer

band compared with the antibody specific to both S866 and S870, confirming reduced phosphorylation of the truncated p100 (**Fig. 2B, 2nd & 3rd panels**).

We further analysed the processing of p100 in Patient 1 compared to his family members (HD 1 and HD 2) with a western blot analysis of cytoplasmic and nuclear lysates of stimulated and unstimulated PBMCs. In the cytoplasmic compartment, we could detect a double band of around 100 kDa in the patient but not in HD1 or HD2. The amount of p52 and RelB present in Patient 1 after CD40L stimulation was similar to the amount present in HD 1 and 2 (**Fig. 2C**), distinct from what we have shown in the whole cell lysates. However, looking at the nuclear compartment, where the transcriptionally competent complex p52/RelB translocated after stimulation[2], we could demonstrate a less strong increase of both p52 and RelB in Patient 1 compared to the controls (**Fig. 2D**). As previously reported, these patients also showed decreased levels of circulating B (**Table S1**) and T follicular helper cells (Tfh – Patient 1, **Fig. S1**), which is characteristic of pathogenic variants in *NFKB2*, leading to an unprocessable p100[4].

These data confirmed that a heterozygous nonsense variant in the NFKB2 protein (p100) resulted in a truncated form p100(p.Tyr868*), which lacks the phosphorylation site S870 and led to a defective p100 processing to p52, resulting in excess of IkB-like activity mediated by the unprocessable p100 and reduced amount of nuclear p52, upon stimulation with CD40L.

Heterozygous *NFKB2* pathogenic variants in CVID are well-documented in the literature and cluster predominantly in exons 22 and 23[4]. In addition to the typical clinical features of CVID (e.g. recurrent respiratory tract infections and hypogammaglobulinaemia), many of the patients have additional features. Klemann *et al* reported 50 patients with CVID and *NFKB2* pathogenic variants, of whom 21 (42%) suffered from ACTH deficiency, and 16 (32%) experienced early-onset alopecia[4]. The two *NFKB2* pathogenic variants at the same position (Patient 1: c.2604C>G;

patient 2: c.2604C>T) that we report in this study have not been previously reported in databases of human genetic variants. However, these pathogenic variants are equivalent to the one described in *Nfkb2*$^{Lym1/+}$ mice (c.2601T>A; p.Tyr867*; CCDS29874.1) with a similar phenotype to our patients (hypogammaglobulinaemia and autoimmunity)[5].

How the disruption of the noncanonical NFκB pathway translates into the clinical phenotype of the patients is unknown and requires further investigation. This pathway is crucial for B cell differentiation into immunoglobulin-producing plasma cells, germinal centre formation, antibody isotype switching and switched memory B cell development[2]. Moreover, when this pathway is activated, it upregulates ICOSL expression on B cells that binds to the costimulatory molecule ICOS on T cells to initiate the differentiation of Tfh cells in germinal centres[2], which is critical for the development of B cell memory. In this context, the frequency of circulating Tfh cells in Patient 1 was significantly less than that in the healthy control (**Fig. S1**), as we and others have shown before[4].

Thus, patients presenting with hypogammaglobulinaemia, recurrent infections, central adrenal insufficiency and autoimmune alopecia should be tested for pathogenic variants in *NFKB2*, by sequencing exons 22 and 23. Confirmatory immunoblots should follow if the *NFKB2* variants are not known to be pathogenic. The use of LCLs should help when cell number is limiting, e.g. in patients with lymphopenia or paediatric cases. Further research into the NFκB pathway in patients with *NFKB2* pathogenic variants and the *Nfkb2*$^{Lym1/+}$ mice will help us better understand the molecular pathogenesis of CVID, as well as B cell malignancies.

ACKNOWLEDGEMENT

We thank King's College Hospital Charitable Trust and Viapath Analytics LLP for funding this study. We thank Dr James Laffan for his help with collating the clinical history of the patients from Epsom & St Helier University Hospitals. We thank Dr Ugo Soffientini and the Institute of Hepatology – King's College Hospital for their continuous support and availability in using their facilities. We are grateful to Mrs Dorota Parsons for her secretarial assistance.

AUTHOR CONTRIBUTIONS

JG, ST, DG-K, IK, GH and MAAI handled clinical aspects of the study and generated clinical data. KS, MF and MAAI designed the research aspects of the study. KS, MF, TH, HM, FS, BC and MAAI generated and analysed research data. KS and MF prepared the figures and the table. KS, MF, ST, NV and MAAI wrote the manuscript. PG and MAAI created the multicolour flow cytometry panel for measuring Tfh frequencies. All authors edited the manuscript.

DISCLOSURE OF CONFLICTS OF INTEREST

None of the authors has any relevant conflict of interest to declare.

REFERENCES

1 Bogaert, D. J. *et al.* Genes associated with common variable immunodeficiency: one diagnosis to rule them all? *J Med Genet* **53**, 575-590 (2016). https://doi.org:10.1136/jmedgenet-2015-103690

2 Sun, S. C. The non-canonical NF-kappaB pathway in immunity and inflammation. *Nat Rev Immunol* **17**, 545-558 (2017). https://doi.org:10.1038/nri.2017.52

3 Liang, C., Zhang, M. & Sun, S. C. beta-TrCP binding and processing of NF-kappaB2/p100 involve its phosphorylation at serines 866 and 870. *Cell Signal* **18**, 1309-1317 (2006). https://doi.org:10.1016/j.cellsig.2005.10.011

4 Klemann, C. *et al.* Clinical and Immunological Phenotype of Patients With Primary Immunodeficiency Due to Damaging Mutations in *NFKB2*. *Front Immunol* **10**, 297 (2019). https://doi.org:10.3389/fimmu.2019.00297

5 Tucker, E. *et al.* A novel mutation in the Nfkb2 gene generates an NF-kappa B2 "super repressor". *J Immunol* **179**, 7514-7522 (2007). https://doi.org:10.4049/jimmunol.179.11.7514

Inborn Errors of Immunity Functional Diagnostics Consortium: a list of members and their affiliations

John Guly [3] (currently at Royal Surrey NHS Foundation Trust, Department of Immunology, Egerton Road, Guildford, GU2 7XX, UK)

Susan Tadros [1,3] (currently at Royal Free Hospital NHS Foundation Trust, Department of Immunology, Pond Street, London, NW3 2QG, UK)

Dorothea Grosse-Kreul[1]

Terrence Hunter [1,2]

Helene Martini [1]

Frances Smith [1,2]

Nisha Verma [1]

Ioasaf Karafotias [1]

Padmalal Gurugama [1] (currently at Cambridge University Hospitals NHS Foundation Trust, Department of Clinical Biochemistry and Immunology, Hills Road, Cambridge, CB2 0QQ, UK)

Barnaby Clark [1] (currently at Precision Medicine, King's College Hospital, Denmark Hill, London SE5 9RS, UK)

LEGENDS TO FIGURES

Figure 1. A. p100 showing the different domains, including Rel homology domain (RHD), nuclear localisation signal (NLS), glycine-rich region (GRR), ankyrin repeat domain (ARD), death domain (DD), cleavage site and p52 fragment following proteolytic degradation (Uniprot: Q00653). The numbers indicate the positions of the amino acid residues. The truncated p100(p.Tyr868*) results from premature termination of translation, deleting the amino acid residues 868-900, including the indicated phospho-serines, rendering p100(p.Tyr868*) unprocessable. The alignment of the indicated sequences shows the three conserved serine residues at positions 866, 870 and 872, with gaps shown as "–". **B.** Sequencing of *NFKB2* exon 23 in the two unrelated affected patients, and as a reference, we used one family member of Patient 1 (part of exon 23 sequence shown, yellow bar indicates nonsense variant). **C.** Family pedigree of Patient 1. Open symbols indicate healthy family members (I-1, I-2, II-2), whereas the black-filled symbol indicates the affected patient (II-1). The arrow points to the proband with a likely *de novo* pathogenic variant.

Figure 2. Immunoblots after cells from Patient 1, HD1 and HD2 were stimulated with CD40L as specified and membranes were probed with the indicated antibodies. **A.** Whole PMBC lysates: increased p52 upon CD40L stimulation in HD1 and HD2 but not in Patient 1 (top panel); a double band around 100kDa in Patient 1 but not in HD1 or HD2 due to a truncated p100 (p.Tyr868*, 93kDa) from the variant allele (top panel); p100 increased upon stimulation in HD1 but not HD2 despite efficient processing to p52 in both; increased phospho-p100 S866/S870 upon CD40L in HDs but not in Patient 1 (2^{nd} panel);. **B.** whole LCL lysates: increased p52 upon CD40L stimulation in HDs but not in Patient 1 (top panel); the truncated p100(p.Tyr868*) is the predominant band visible in Patient 1 (top panel); increased p100 upon CD40L stimulation in HD1, but no change in p100 in HD2 (top panel); both HD1 and HD2 show efficient p100

processing to p52 upon CD40L stimulation (top panel); increased phospho-p100 upon CD40L in HDs but less so in Patient 1 (second & third panels). **C.** Cytoplasmic PBMC lysates: no difference in bands between Patient 1 and HDs except that Patient 1 has a double band around 100kDa (top panel). **D.** Nuclear PBMC lysates: less increase in nuclear p52 in Patient 1 compared with HDs reflecting reduced processing of p100 in the patient (tope panel). Immunoblots shown are from the same experiment with the membrane stripped and re-probed with antibodies. Bar charts represent quantification of the relative density of bands by digital densitometry, normalised to the loading control as follow:

$$Density\ of\ Target\ Protein \times \frac{Density\ of\ Loading\ Control\ in\ Control\ Sample\ Lane}{Density\ of\ Loading\ Control\ in\ Target\ Protein\ Lane}$$

FIG. 1A

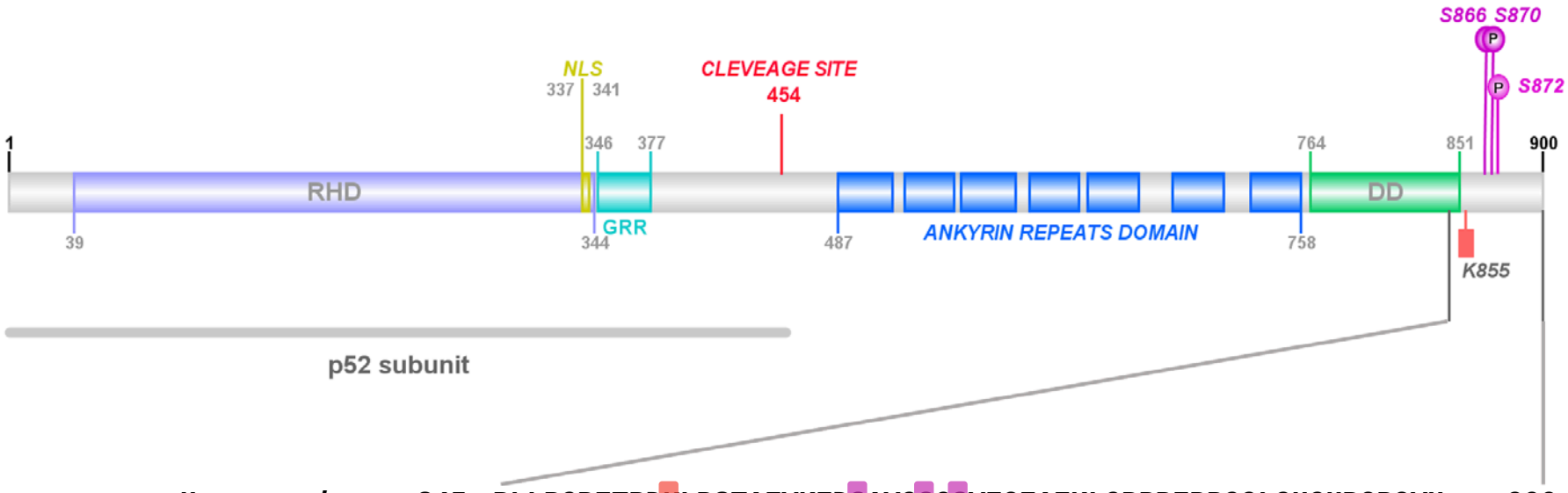

Homo sapiens	845	RLLRGPETRDKLPSTAEVKEDSAYGSQSVEQEAEKLGPPPEPPGGLCHGHPQPQVH	900
Homo sapiens (p.Tyr868*)	845	RLLRGPETRDKLPSTAEVKEDSA*----------	867
Mus musculus	845	RLLRGPETRDKLPST-EVKEDSAYGSQSVEQEAEKLCPPPEPPGGLCHGHPQPQVH	899
Mus musculus (Lym1)	845	RLLRGPETRDKLPST-EVKEDSA*----------	866
Oryctolagus cuniculus	845	RLLRGPETRDKLPST-EVKEDSAYGSQSVEQEAEKLGPPPEPPGGLCHGHPQPQVH	899
Bos taurus	846	RLLKGPETQEKLPSTAEVKEDSAYGSQSVEQETEKLGPPPEPPGGLCHGRPQPQVH	901
Canis lupus familiaris	845	RLLRGPEARDKLPSTAEVKEDSAYGSQSVEQEAEKLGSPPEPPGGLCHGHPQPQVH	900
Xenopus tropicalis	899	ELLCKSETYAKHQSPAEGKNDSAYESQSMEVDQSSAELSPTTEPAIGQ	946
Danio rerio (zebrafish)	863	RLLRDSQPREDKQS-SDSTEDSGFGSQSIGEEMANPAVGNH	902

FIG.1B

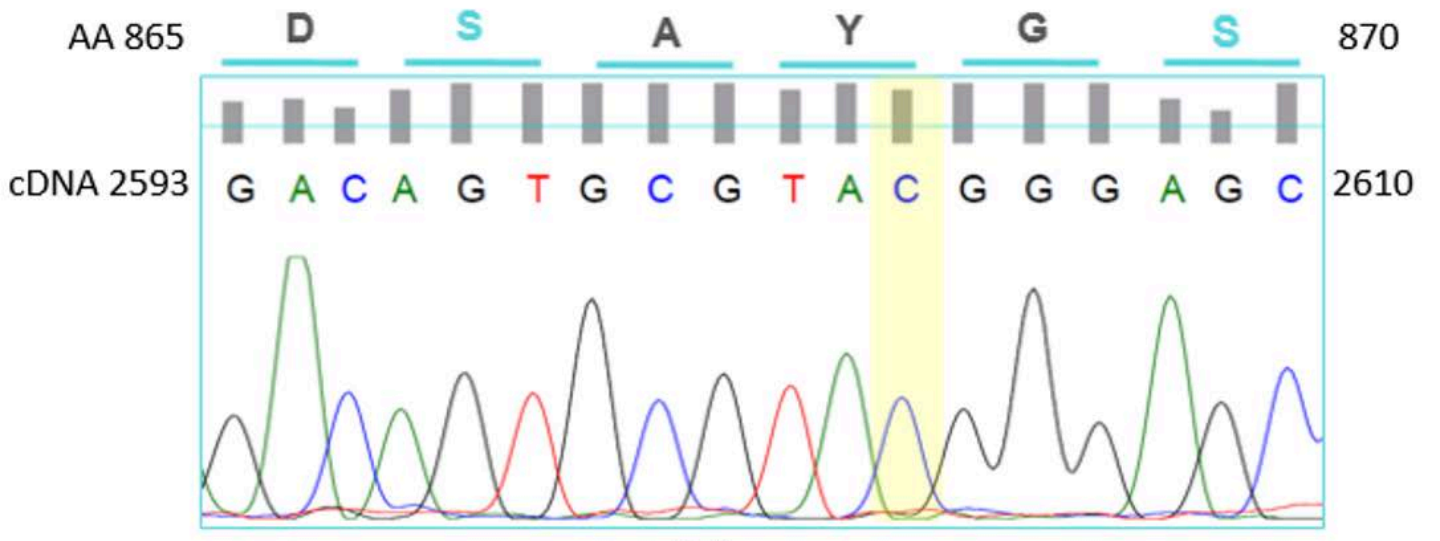

Reference

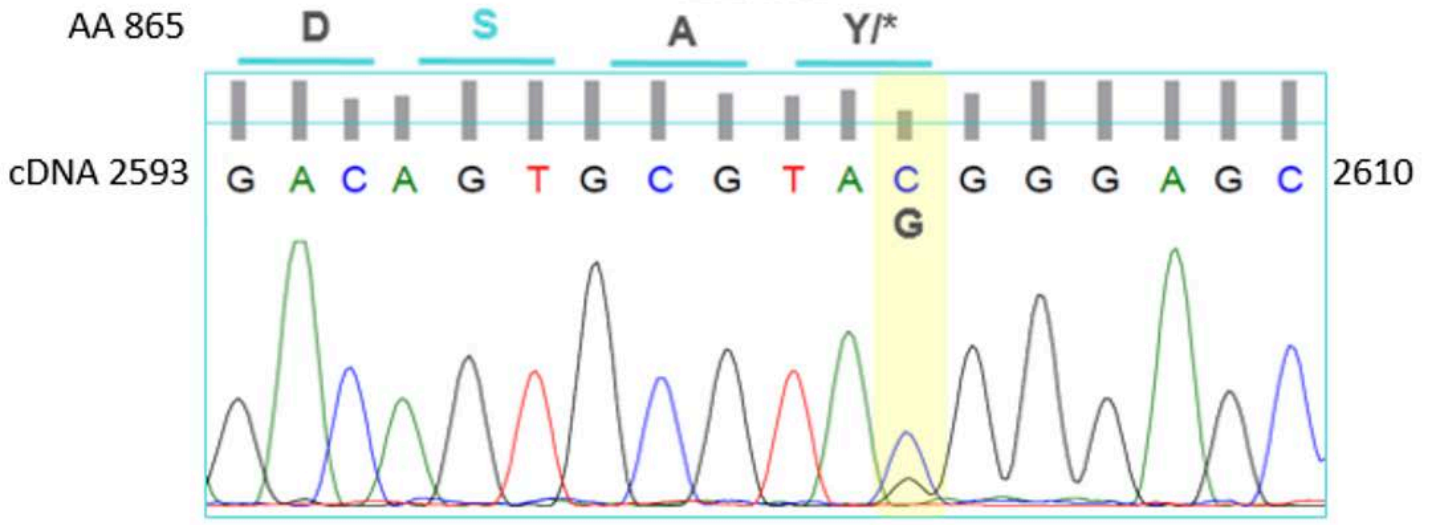

Patient 1 c.2604C>G; p.Tyr868*

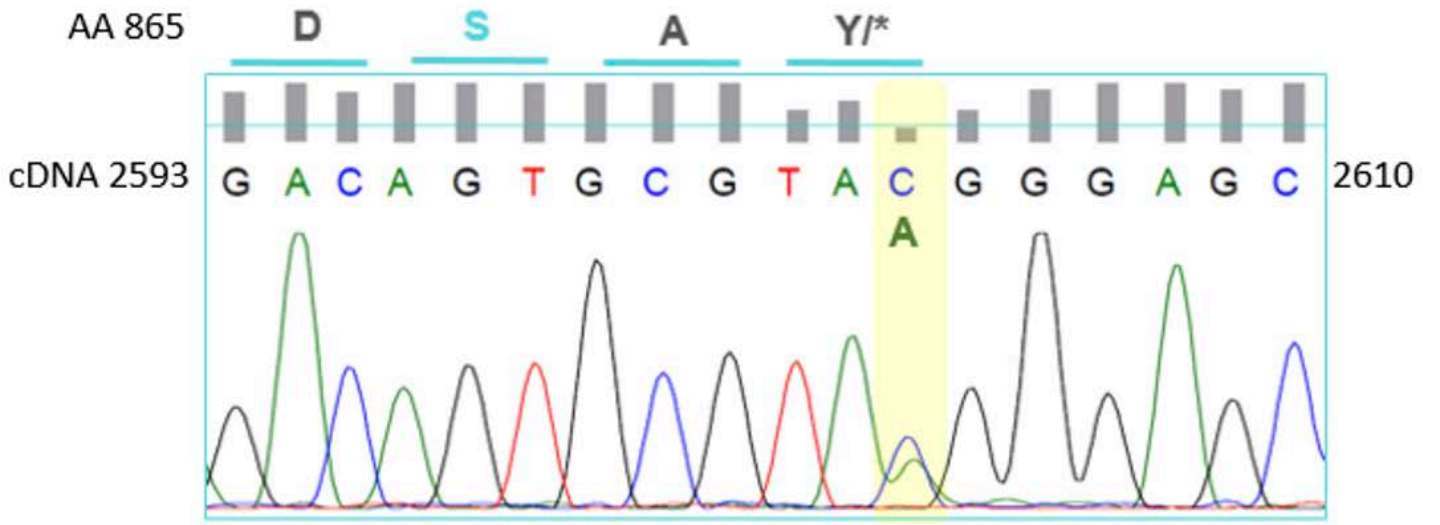

Patient 2 c.2604C>A; p.Tyr868*

FIG. 1C

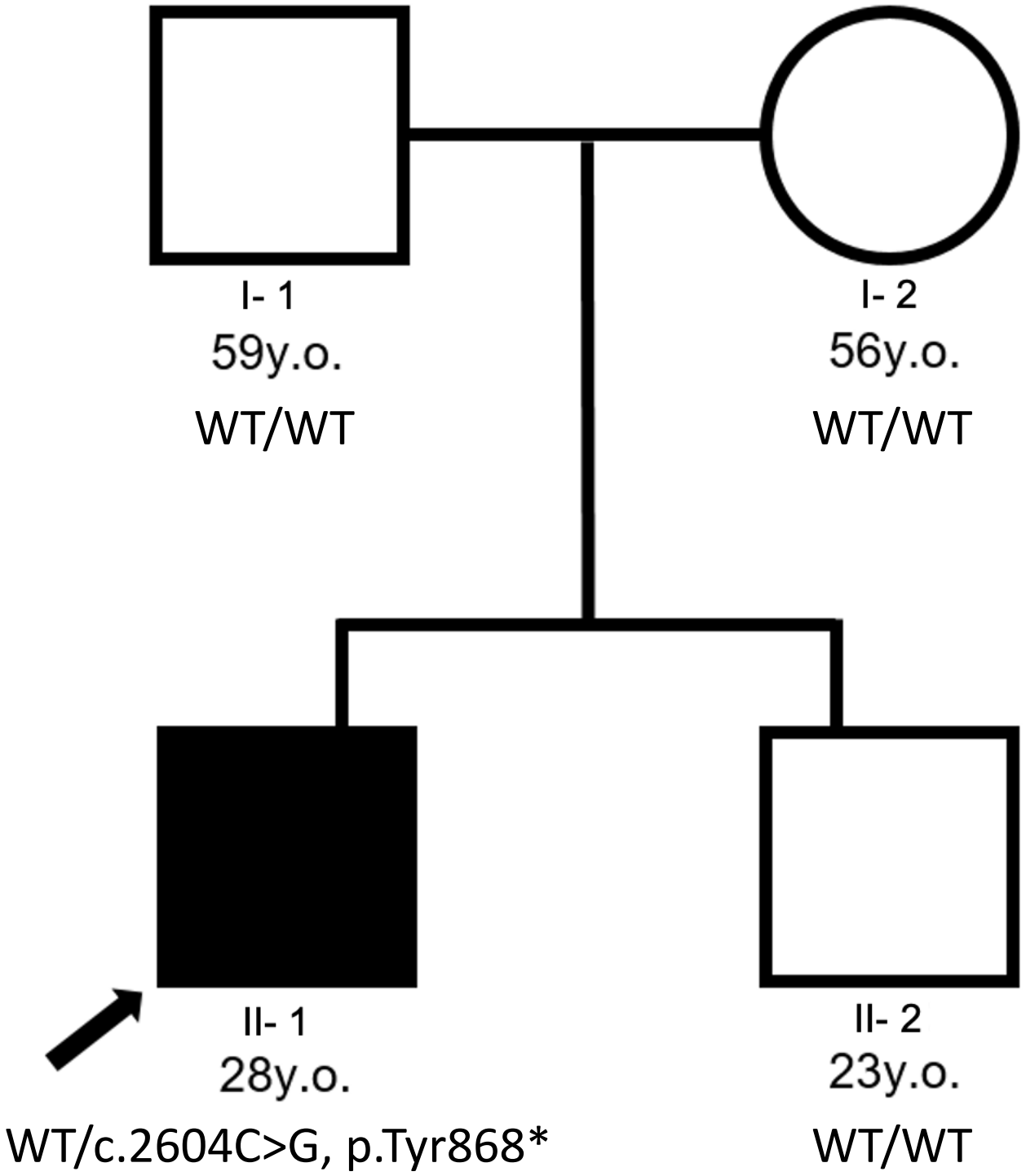
I- 1
59y.o.
WT/WT
I- 2
56y.o.
WT/WT
II- 1
28y.o.
WT/c.2604C>G, p.Tyr868*
II- 2
23y.o.
WT/WT

FIG. 2A

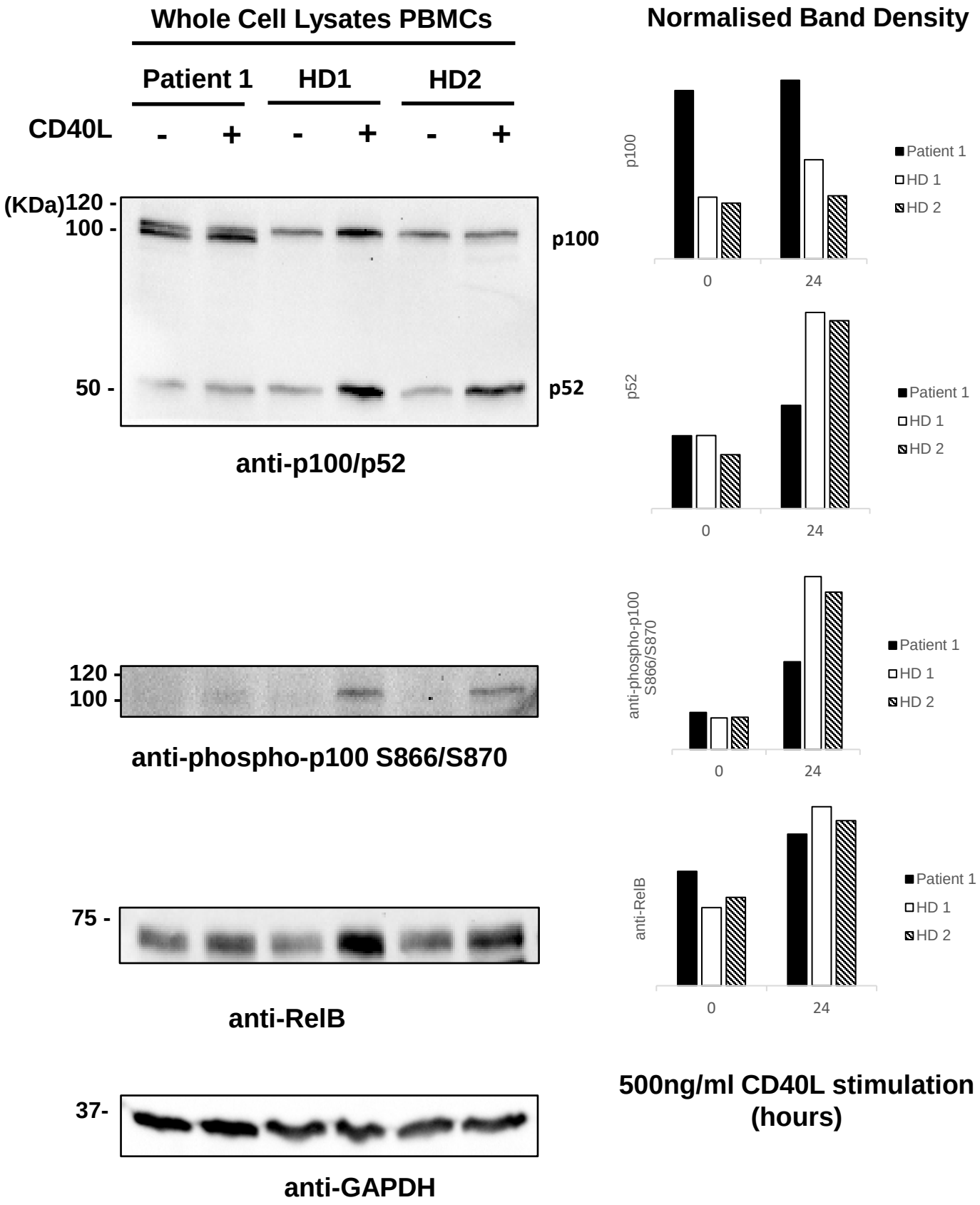
Whole Cell Lysates PBMCs
Patient 1
HD1
HD2
CD40L
- + - + - +
(KDa)120 -
100 -
50 -
p100
p52
anti-p100/p52
120 -
100 -
anti-phospho-p100 S866/S870
75 -
anti-RelB
37-
anti-GAPDH
Normalised Band Density
p100
p52
anti-phospho-p100 S866/S870
anti-RelB
Patient 1
HD 1
HD 2
0
24
500ng/ml CD40L stimulation (hours)

FIG. 2B

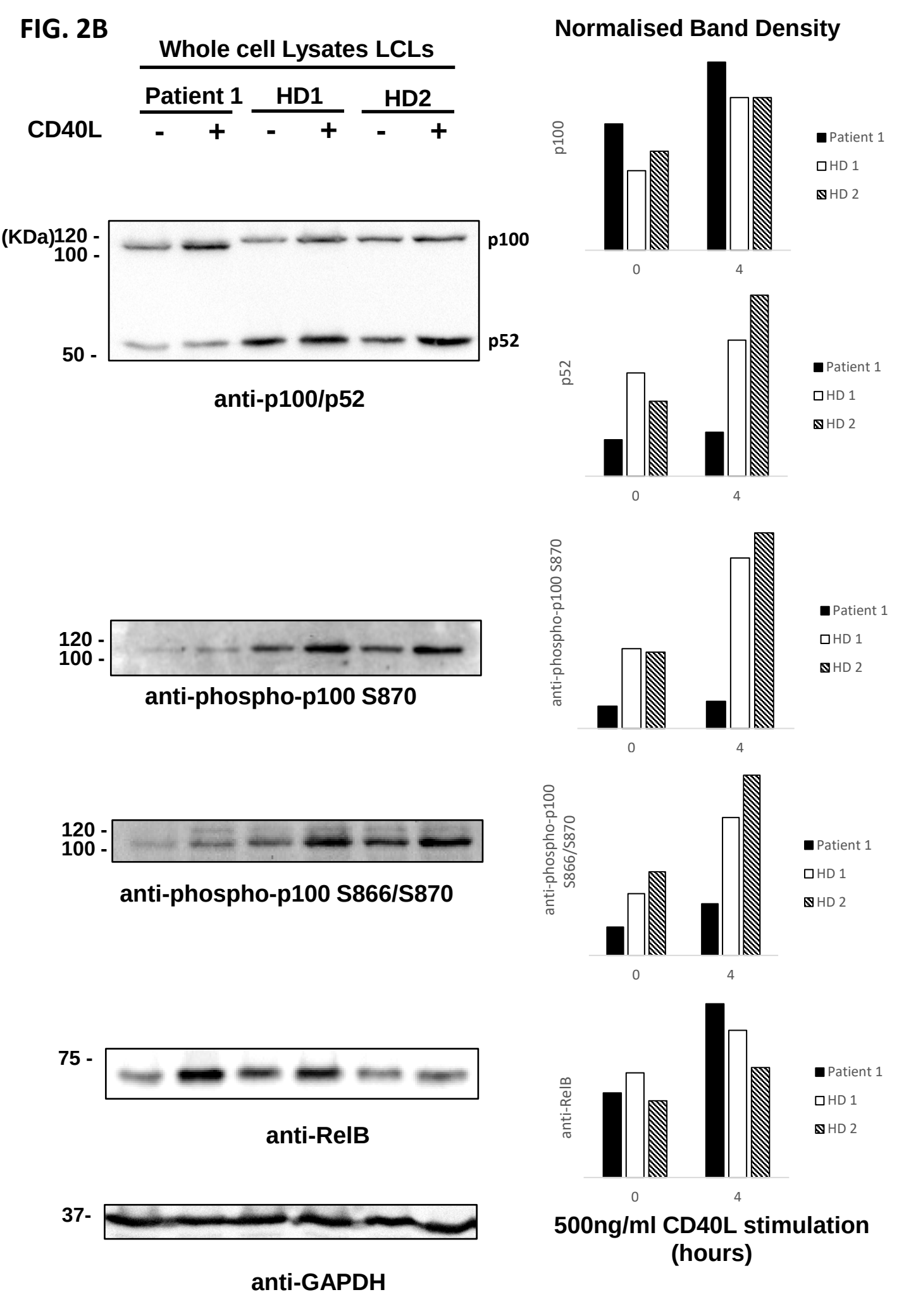
Whole cell Lysates LCLs
Patient 1
HD1
HD2
CD40L
- + - + - +
(KDa)120 -
100 -
50 -
p100
p52
anti-p100/p52
120 -
100 -
anti-phospho-p100 S870
120 -
100 -
anti-phospho-p100 S866/S870
75 -
anti-RelB
37-
anti-GAPDH
Normalised Band Density
p100
p52
anti-phospho-p100 S870
anti-phospho-p100 S866/S870
anti-RelB
Patient 1
HD 1
HD 2
0
4
500ng/ml CD40L stimulation (hours)

FIG. 2C

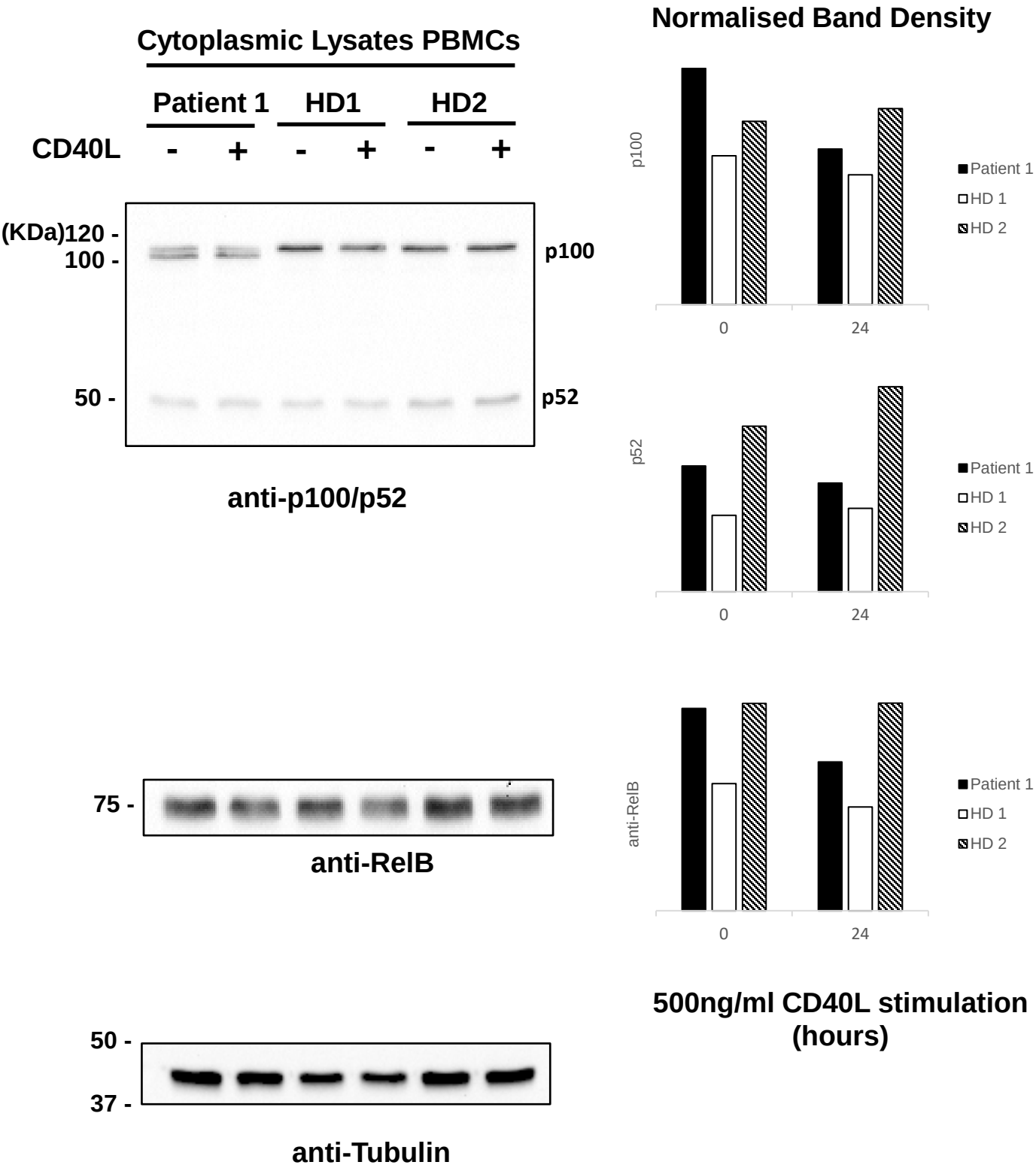
Cytoplasmic Lysates PBMCs
Patient 1
HD1
HD2
CD40L
- + - + - +
(KDa)120 -
100 -
50 -
p100
p52
anti-p100/p52
75 -
anti-RelB
50 -
37 -
anti-Tubulin
Normalised Band Density
p100
p52
anti-RelB
Patient 1
HD 1
HD 2
0
24
500ng/ml CD40L stimulation (hours)

FIG. 2D

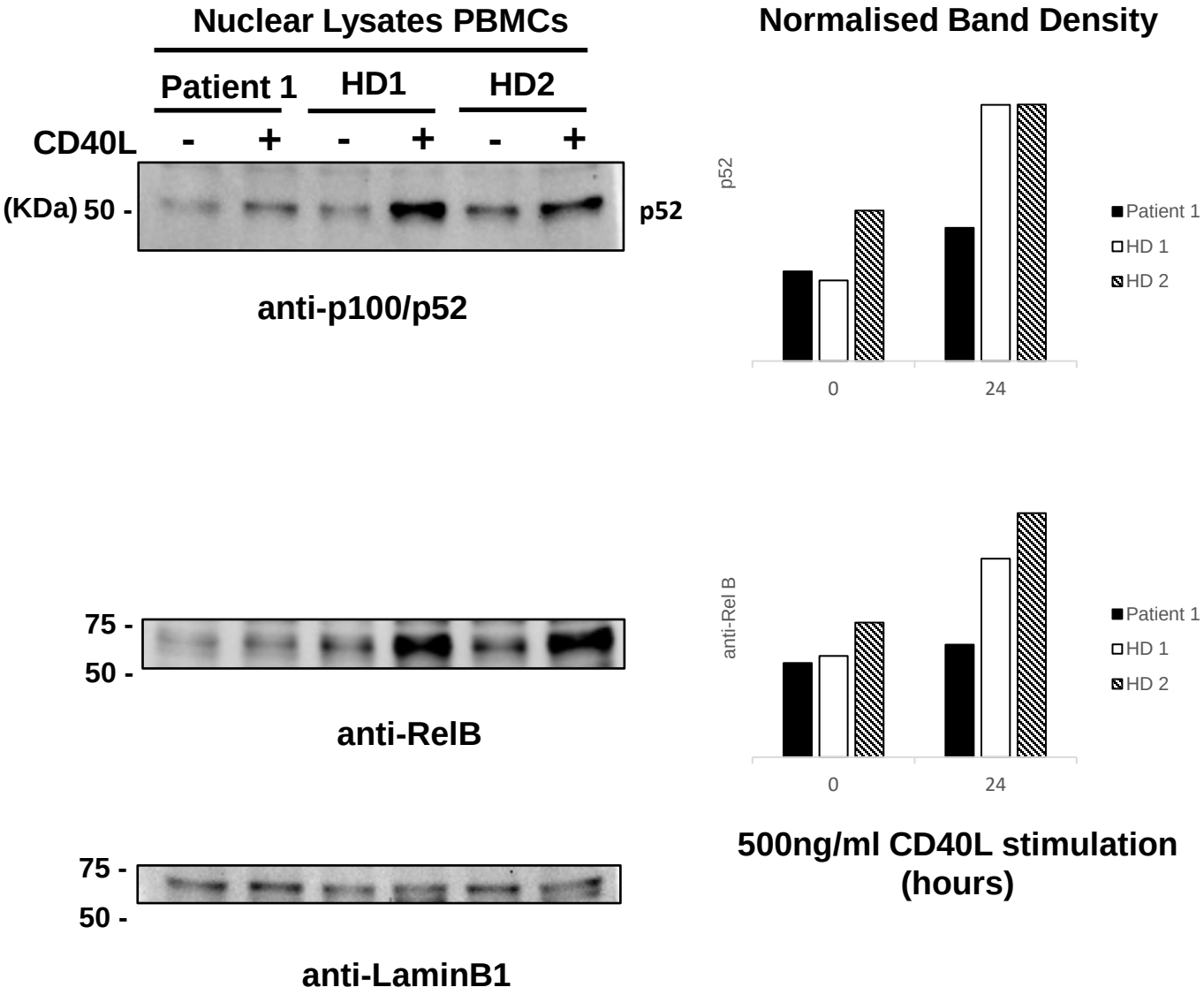
Nuclear Lysates PBMCs
Patient 1
HD1
HD2
CD40L
- + - + - +
(KDa)
50 -
p52
anti-p100/p52
75 -
50 -
anti-RelB
75 -
50 -
anti-LaminB1
Normalised Band Density
p52
Patient 1
HD 1
HD 2
0
24
anti-Rel B
Patient 1
HD 1
HD 2
0
24
500ng/ml CD40L stimulation (hours)

METHODS

Dye Terminator sequencing

Extracted DNA (100 ng/µl) from whole blood samples was added to a PCR reaction (1.5mM MgCl2) containing primers (NFKB2-F: 5′-TGTAAAACGACGGCCAGTGGTCCAGAAACCCGAGACAA-3′; NFKB2-R: 5′-CAGGAAACAGCTATGACCGAAATAGGTGGGGACGCTGT-3′) to amplify the exon 23 of *NFKB2*. The PCR amplification cycles were as follows: 94°C for 30 sec; 64°C for 30 sec; and 72°C for 40 sec; for 35 cycles. Amplification was confirmed using agarose gel electrophoresis, and PCR products were cleaned-up for cycle sequencing using the Biomek NXP® and the Agencourt AMPure XP® reagents (Beckman Coulter). Cycle sequencing was carried out using the BigDye® Terminator V3.1 cycle sequencing kit (Life Technologies) using M13 primers with sequences complementary to the underlined regions of the amplification primers, and the products were purified using the Biomek NXP® and the Agencourt CleanSEQ® reagents (Beckman Coulter). Sequence products were run on the ABI 3130 xl Genetic Analyser (Life Technologies) and analysed using Sequencher Software v4.1.4 (GeneCodes USA). The sample traces were compared to a sequence downloaded from UCSC Genome Browser (http://genome.ucsc.edu/), chr10:104154229-104162281 (Hg19).

Cell Culture

Peripheral blood mononuclear cells (PBMCs) and Lymphoblastoid cell lines (LCLs) derived from Epstein-Barr virus (EBV)-transformed PBMCs were maintained in complete RPMI-1640 with 2 mM L-glutamine, 10% fetal bovine serum, penicillin (100 U/ml), and streptomycin (100 mg/ml) in climate controlled CO_2 incubator at 37°C

Immunoblotting

PBMCs were isolated by using Ficoll-Hypaque density centrifugation. $7x10^6$ PBMCs/sample or $5x10^6$ LCLs/sample were activated with MEGACCD40L (Enzo Life Sciences) for either 24h (PBMCs) or 4h (LCLs) in 12-well plate in a climate-controlled CO_2 incubator at 37°C. Whole cell lysates were prepared using 1% Nonidet –P40 in 150mM NaCl and 50mM Tris (pH 8) in presence of protease and phosphatase inhibitor cocktail mix (Sigma-Aldrich). The lysates were incubated on ice for 5 minutes and centrifuged at 16,000g for 10 minutes. The lysates were transferred to a new Eppendorf tube and total protein in each sample was determined using Pierce BCA Protein Assay kit (Thermofisher Scientific). Alternatively cytoplasmic and nuclear cell lysates we generated using NE-PER nuclear and cytoplasmic Extraction Reagents (Thermofisher Scientific). The lysates (30µg per lane - whole and cytoplasmic; 20µg per lane – nuclear) were resolved by SDS-PAGE and transferred to an Immobilon FL PDVF membrane (Merck-Millipore). The membranes were blocked with either 5% nonfat-dried milk or 5% bovine serum albumin (BSA) in TBS 0.1% tween and incubated overnight at 4°C with the primary antibody. NFKB2 p100/p52 antibody (Cat.4882), phospho-NFKB2p100 (S866/870) antibody (Cat.4810), RelB (Cat.4922), LaminB1 (Cat.134355), α-Tubulin (Cat.2144) were from Cell Signaling Technology,phospho-NFKB2p100 (S870) antibody was from Thermo

Fisher Scientific (Cat. PA5-37663) and GAPDH was from Abcam (Cat.ab181602). Immunoblots were carried out using either peroxidase-labelled secondary antibody (Cat.7074) from Cell Signaling Technology or ECL anti-Rabbit IgG (Cat.NA934V) from Merck and SuperSignal West Pico Plus chemiluminescent substrate (Cat.34580) from Thermofisher Scientific. Images were acquired using ChemiDoc XRS+ (Bio-Rad). Densitometric analysis of the immunoblots digital images were performed with Image Studio Lite software (version 5.2) (Li-cor) and images were also modified using ImageJ (NIH).

Membranes were stripped in order to be re-probed with a different antibody using Restore Plus western blot Stripping Buffer (Cat.21059) from Thermofisher Scientific.

Precision Plus Protein Kaleidoscope Prestained Proteins Standards (Cat.1610365) was purchased from Bio-rad and MagicMark XP Western Protein Standard (Cat.LC5602) from Thermofisher Scientific.

Flow cytometry

Peripheral whole blood samples were collected and stained within 48 hours from collection. 200 µl of whole blood was stained with a mixture of the following antibodies at optimal concentration: CD3-APC/A700 (Beckman Coulter), CD4-Krome Orange (Beckman Coulter), CXCR5-APC (R&D Systems), and CD45RA-APC/A750 (Beckman Coulter). Samples were incubated at 2-8°C for 30 minutes in darkness. IOTest 3 10X fixative solution (Beckman Coulter) and Versalyse lysing solution (Beckman Coulter), previously mixed as per manufacturer instructions, were added to the samples, followed by 10 minutes incubation at room temperature, protected from light. The samples were then centrifuged at 2000 RPM for 5 minutes and the supernatant was removed by aspiration. A minimum of 50,000 $CD3^+$ T cells were acquired with Gallios flow cytometer (Beckman Coulter) and analysed with Kaluza software version 1.5 (Beckman Coulter).

Table S1: Salient clinical characteristics and laboratory findings of the two unrelated patients with *NFKB2* heterozygous mutations.

Patients[a]	**Patient 1**	**Patient 2**
Sex	Male	Female
Age at Evaluation	26 years	36 years
Infections	• Recurrent otitis media, and • chest infections Scarring after varicella zoster virus infection Two episodes of pneumococcal meningitis Chronic sinusitis Bronchiectasis	Recurrent urinary and respiratory tract infections Orbital cellulitis Recurrent conjunctivitis Impetigo Perineal candidiasis Perineal and cutaneous Herpes Simplex Viral infections (HSV-1)
Autoimmunity	Eczema Alopecia areata Dystrophic nails	Vitiligo Alopecia universalis Dystrophic nails
Treatment	Immunoglobulin and hydrocortisone replacement therapy	Immunoglobulin replacement therapy
Subjects	**Patient 1**	**Patient 2**
Full Blood Count		
Haemoglobin (115 – 155 g/L)	151	116
Platelets (150 – 450 × 10^9/L)	280	410
Neutrophils (2.2 – 6.3 × 10^9/L)	11.3	7.4
Immunoglobulins (Ig)		
IgG (6.34 – 18.11 g/L)	1.50↓ *	9.30 †
IgA (0.87 – 4.12 g/L)	<0.23↓ *	<0.23↓ †
IgM (0.53 – 2.23 g/L)	<0.18↓ *	<0.18↓ †
Vaccination Serology		
Haemophilus influenzae type b antibodies (> 0.14 mg/L)	2.14 †	NA
Tetanus antibodies (> 0.14 IU/mL)	2.89 †	NA
Serotype-specific pneumococcal antibodies (IgG > 1.5 µg/mL against 50% or more of serotypes tested)	35 †	NA
Lymphocyte Subsets		
Lymphocytes (1300 – 4000 × 10^6/L)	1300	1100 ↓
CD3+ (723 – 2737 × 10^6/L)	1110	1010
CD4+ (404 – 1612 × 10^6/L)	860	610
CD8+ (220 – 1129 × 10^6/L)	240	370
CD16+ CD56+ NK cells (84 – 724 × 10^6/L)	120	120
CD19+ (80 – 616 × 10^6/L)	40↓	80
Autoantibodies	ND	Neg

Reference intervals according to Viapath medical laboratories.

*, before immunoglobulin replacement
†, after immunoglobulin replacement
NA, not available;
ND, not done;
Neg, negative;
NK, natural killer.

Figure S1: Frequency of T follicular helper cells in unrelated healthy control and affected patient 1.

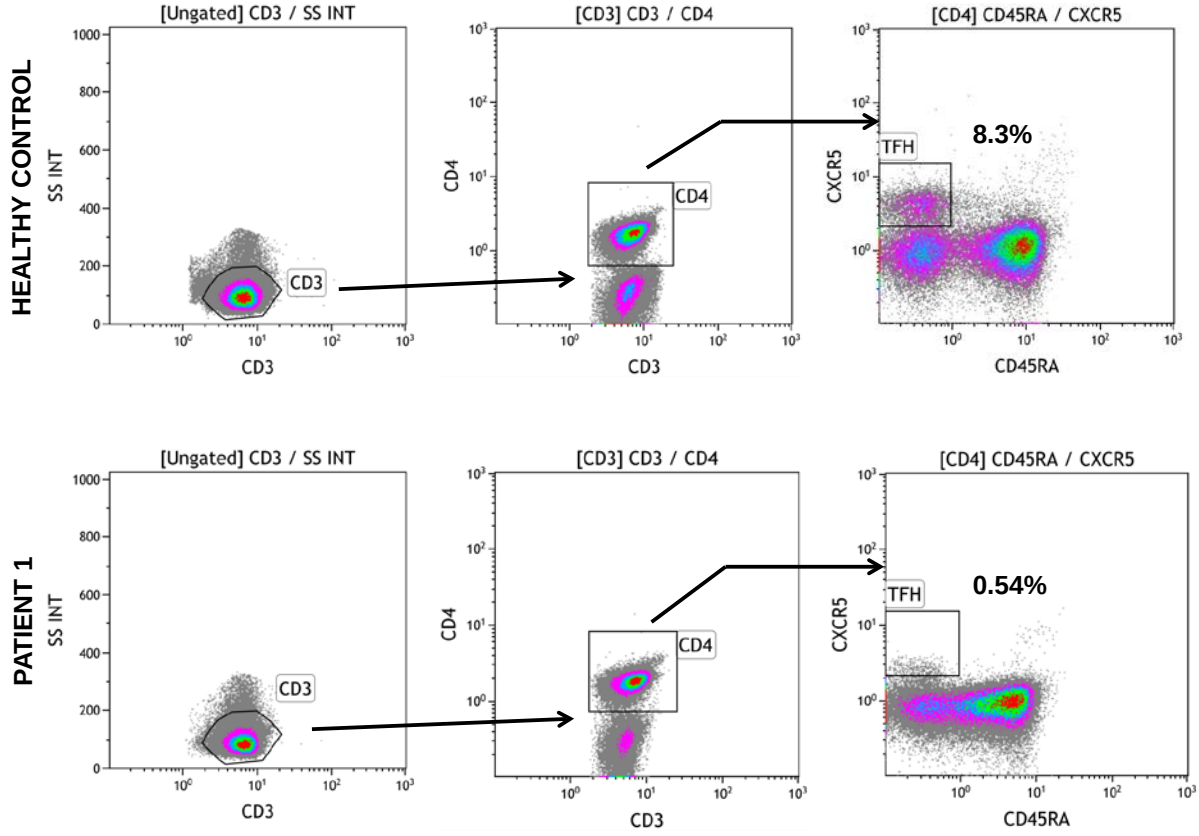

Figure S1. Reduced circulating Tfh frequencies in the affected patient 1 with the *NFKB2* mutation compared to an unrelated healthy control. Total circulating Tfh frequencies were measured using flow cytometry. Peripheral whole blood samples were collected and stained for CD3 (T cell marker), CD4 (Helper T cell marker), CD45RA (Naïve T cell marker) and CXCR5 (Tfh marker). Arrows represent gating strategy. Tfh population was defined as $CD3^{+}$ $CD4^{+}$ $CD45RA^{-}$ $CXCR5^{+}$ cells. Data is representative of three experiments.